Angular Distributions From (d,^{2}He) Reactions

Gulnara Ajupova and C.A. Gagliardi

With the Proton Spectrometer Monte Carlo functional, we were able to create angular distributions for the 125 MeV ^{54}Fe data and 140 MeV data on light targets.

The cross-sections from neighboring spectrometer angles were tested for an agreement in the overlap region. From this, we concluded that the Monte-Carlo solid angle calculations are reliable in the range (-5E,+4E) around the central ray.

The cross-section angular distributions were fitted with the theoretically calculated cross-sections of Gamow-Teller and spin-dipole states using the DWUCK4 program. The optical potential parameters of the entrance and exit channel were chosen to be the same, obtained in the analysis of elastic scattering cross-sections of 110 MeV and 120 MeV deuterons off of ^{12}C, ^{58}Ni and ^{208}Pb [1]. The potential has the general form:

$$V(r) = -V_R\ f(r,r_0,a_0) - iW_S\ f(r,r_I,a_I) + \\ + i4\,(a_I)^2 W_D\,(d/dr)\,f(r,r_I,a_I) + \\ + V_{LS}\,(\lambda_B)^2\,(L\,S)\,(1/r)(d/dr)\,f(r,r_{LS},a_{LS}) + \\ + V_{Coul}, \qquad (1)$$

where $f(x,y,z)$ is a standard Woods-Saxon form, and λ_B is pion Compton wavelength.

For the targets with $A \leq 24$ at both energies we chose the optical parameters of the best fit for 120 MeV deuterons on carbon. To achieve a fit for the ^{54}Fe target we had to use the optical potential parameters obtained for 120 MeV deuterons on ^{58}Ni.

The fits to the Gamow-Teller states were able to reproduce the shape of the cross-sections quite well with leading contribution from ΔL=0 reaction together with a small but non-negligible contribution from ΔL=2 component, especially the forward peak characteristic of the direct transfer reaction. The ΔL=2 contribution was necessary to fill in the diffractive minima of the calculated DWBA pure Gamow-Teller cross-section.

Figure 1 shows the angular distributions and their DWBA fits for ground and first excited states populated in ^{12}C(d,^{2}He)^{12}B reactions at 140.45 MeV (left) and 124.78 MeV (right). The ground state cross-sections are in the top panels.

At the larger scattering angles, the cross-sections were systematically lower than DWBA prediction. The angle where this discrepancy begins to show is dependent on target mass and energy. Consistently, the data taken at E_d=140.45 MeV showed good agreement in range $\leq$18E, whereas ^{12}C data at E_d=124.78 MeV was good up to 19E. The ^{54}Fe data extends only to 15E and therefore we cannot draw any conclusions about how the fit quality depends on energy. The only exception here was the cross-section of the very light ^{6}Li at E_d=140.45 MeV. Its cross-section decreases much faster than DWBA prediction. Most probably, this problem is an indication of the

contribution of the more complex reaction mechanism.

The good fits were achieved with a combination of attractive central Yukawa and tensor pion-exchange terms with similar strength. The sign of the integral of the tensor contribution needed to be opposite to that of the central piece.

To show that cross-sections do not strongly depend on the optical potential parameters of the entrance and exit channels, we also performed the fits with optical potential parameters of the relativistic Daehnick 79 DCV, F global fit with appropriate mass and energy values [2]. For light nuclei the Daehnick fits were as good as with our custom fits. For lower energy ^{54}Fe data set the Daehnick DWBA cross-section is slightly worse. Both sets of potential parameters are listed in the Table I.

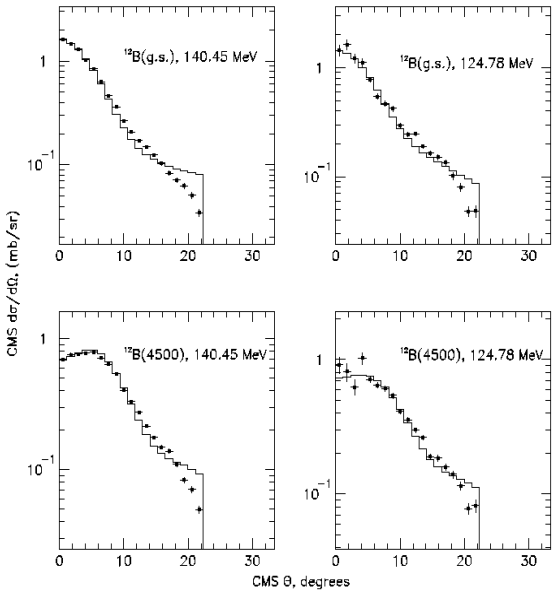

Figure 1. The angular distributions (points with errors) and DWBA fits (curves).

Table I. Optical Potential Parameters for DWBA fits.

TGT,E_{lab}	^{6}Li,140	^{12}C,140	^{13}C,140	^{24}Mg,140	^{12}C,125	A=6-24	^{54}Fe,125	^{54}Fe
V_R	49.71	50.56	50.50	51.91	54.99	55.48	58.74	59.11
r_0	1.17	1.17	1.17	1.17	1.17	1.16	1.17	1.14
a_0	0.89	0.89	0.89	0.89	0.87	0.78	0.87	0.84
W_S	14.08	14.08	14.08	14.08	12.52	6.99	12.52	12.24
W_D	2.27	2.27	2.27	2.27	3.34	1.50	3.34	1.55
r_I	1.26	1.26	1.26	1.26	1.26	1.33	1.26	1.28
a_I	0.65	0.67	0.65	0.72	0.67	0.79	0.74	0.82
r_C	1.30	1.30	1.30	1.30	1.30	1.30	1.30	1.30
V_{LS}	2.71	2.71	2.71	2.71	3.21	4.14	3.21	6.36
r_{LS}	1.07	1.07	1.07	1.07	1.07	1.42	1.07	1.18
a_{LS}	0.66	0.66	0.66	0.66	0.66	0.83	0.66	0.89
From ref.	[2]	[2]	[2]	[2]	[2]	[1]	[2]	[1]

References

1. A.C. Betker, C.A. Gagliardi, D.R. Semon, R.E. Tribble, H.M. Xu, and A.F. Zaruba, Phys. Rev. C **48**, 2085 (1993).

2. W. W. Daehnick, J.D. Childs, and Z. Vrjcelj,
Phys. Rev. C **21**, 2253 (1980).